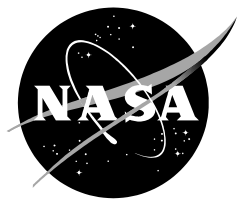


NASA/TM-2012-216006



Modeling of Aerobrake Ballute Stagnation Point Temperature and Heat Transfer to Inflation Gas

Parviz A. Bahrani
NASA Ames Research Center
Moffett Field, California

March 2012

The NASA STI Program Office . . . in Profile

Since its founding, NASA has been dedicated to the advancement of aeronautics and space science. The NASA Scientific and Technical Information (STI) Program Office plays a key part in helping NASA maintain this important role.

The NASA STI Program Office is operated by Langley Research Center, the Lead Center for NASA's scientific and technical information. The NASA STI Program Office provides access to the NASA STI Database, the largest collection of aeronautical and space science STI in the world. The Program Office is also NASA's institutional mechanism for disseminating the results of its research and development activities. These results are published by NASA in the NASA STI Report Series, which includes the following report types:

- **TECHNICAL PUBLICATION.** Reports of completed research or a major significant phase of research that present the results of NASA programs and include extensive data or theoretical analysis. Includes compilations of significant scientific and technical data and information deemed to be of continuing reference value. NASA's counterpart of peer-reviewed formal professional papers but has less stringent limitations on manuscript length and extent of graphic presentations.
- **TECHNICAL MEMORANDUM.** Scientific and technical findings that are preliminary or of specialized interest, e.g., quick release reports, working papers, and bibliographies that contain minimal annotation. Does not contain extensive analysis.
- **CONTRACTOR REPORT.** Scientific and technical findings by NASA-sponsored contractors and grantees.

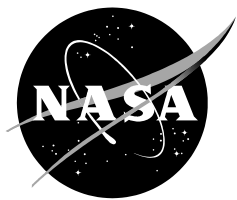
- **CONFERENCE PUBLICATION.** Collected papers from scientific and technical conferences, symposia, seminars, or other meetings sponsored or cosponsored by NASA.
- **SPECIAL PUBLICATION.** Scientific, technical, or historical information from NASA programs, projects, and missions, often concerned with subjects having substantial public interest.
- **TECHNICAL TRANSLATION.** English-language translations of foreign scientific and technical material pertinent to NASA's mission.

Specialized services that complement the STI Program Office's diverse offerings include creating custom thesauri, building customized databases, organizing and publishing research results . . . even providing videos.

For more information about the NASA STI Program Office, see the following:

- Access the NASA STI Program Home Page at <http://www.sti.nasa.gov>
- E-mail your question via the Internet to help@sti.nasa.gov
- Fax your question to the NASA Access Help Desk at (301) 621-0134
- Telephone the NASA Access Help Desk at (301) 621-0390
- Write to:
NASA Access Help Desk
NASA Center for AeroSpace Information
7115 Standard Drive
Hanover, MD 21076-1320

NASA/TM-2012-216006



Modeling of Aerobrake Ballute Stagnation Point Temperature and Heat Transfer to Inflation Gas

Parviz A. Bahrani
NASA Ames Research Center
Moffett Field, California

National Aeronautics and
Space Administration

Ames Research Center
Moffett Field, California 94035-1000

March 2012

Available from:

NASA Center for AeroSpace Information
7115 Standard Drive
Hanover, MD 21076-1320
(301) 621-0390

National Technical Information Service
5285 Port Royal Road
Springfield, VA 22161
(703) 487-4650

TABLE OF CONTENTS

SUMMARY	1
INTRODUCTION	1
AEROCAPTURE BALLUTES	2
BALLUTE THERMAL PROBLEM	3
THERMAL MODEL	4
TRAJECTORY FOR AEROCAPTURE	7
HEAT TRANSFER RESULTS	7
VERIFICATION	9
CONCLUSIONS	9
BIBLIOGRAPHY	10

LIST OF FIGURES

- Figure 1. Schematic representation of the spacecraft-ballute system
Figure 2. Free-stream velocity as a function of time from the initial conditions
Figure 3. Convective heat transfer as a function of time
Figure 4. Membrane temperature at the stagnation point
Figure 5. Bulk temperature of the inflation gas

NOMENCLATURE

- α = thermal diffusivity of inflation gas, $k / \rho c_p$, m^2/s
 σ = Stefan-Boltzmann constant, $5.729 \times 10^{-8} W/m^2 K^4$
 ε = emissivity of Ballute
 k = thermal conductivity of inflation gas, $W/m K$
 q_a = convective heat flux, W/m^2
 q_c = inflation gas conduction heat flux, W/m^2
 T_∞ = temperature of free stream, K
 T_w = membrane temperature, K
 T_i = inflation gas initial temperature, K
 T_b = inflation gas bulk temperature, K
 c_p = heat capacity of inflation gas, $Joules/kg K$
 U_∞ = free stream velocity, m/s
 r = radius of Ballute ring, m
 ρ = inflation gas density, kg/m^3
 ρ_∞ = free stream density, kg/m^3
 Δt = time step, s
 n = time step index

Modeling of Aerobrake Ballute Stagnation Point Temperature and Heat Transfer to Inflation Gas

PARVIZ A. BAHRAMI

NASA AMES RESEARCH CENTER
MOFFETT FIELD, CALIFORNIA

SUMMARY

A trailing ballute drag device concept for spacecraft aerocapture is considered. A thermal model for calculation of the ballute membrane temperature and the inflation gas temperature is developed. An algorithm capturing the most salient features of the concept is implemented. In conjunction with the thermal model, trajectory calculations for two candidate missions, Titan Explorer and Neptune Orbiter missions, are used to estimate the stagnation point temperature and the inflation gas temperature. Radiation from both sides of the membrane at the stagnation point and conduction to the inflating gas are included. The results showed that the radiation from the membrane and to a much lesser extent conduction to the inflating gas, are likely to be the controlling heat transfer mechanisms and that the increase in gas temperature due to aerodynamic heating is of secondary importance.

INTRODUCTION

NASA's Science Mission Directorate in recent years has supported basic research and technology investigations for advanced space propulsion through its In-Space Propulsion (ISP) office as part of the Solar System Exploration Program. The goal is to develop technologies that support reduced trip time with increased payload capabilities, while reducing the costs associated with propulsion systems applicable to earth orbit, planetary and interstellar deep space applications. The intent is to identify, advance, and mature technologies that enable NASA exploration missions to the outer planets.

Research to develop critical technologies for aerocapture provides the impetus for the present work. Aerocapture is a spacecraft flight maneuver performed upon arrival at a planet. It utilizes the atmospheric drag to decelerate the spacecraft for capture by the planet's gravity into orbit during a single pass. Aerocapture can significantly reduce mission mass and cost in comparison to conventional orbital insertion methods [1].

The aerocapture maneuver can be accomplished with two basic types of systems. The spacecraft can be covered with thermal protection material or the vehicle deploy an aerocapture device, such as an inflatable heat shield or an inflatable trailing ballute, a combination balloon and parachute made of thin, durable material towed behind the vehicle. The former is a variation of the conventional aeroshell, using low mass and low thermal conduc-

tivity materials with sufficient thermal and mechanical properties to allow orbital insertion. The aeroshell can accommodate aerodynamic control to overcome atmospheric uncertainties and initial entry conditions, while protecting the payload from hypersonic aerothermal heating. The present research is concerned with the latter technique, inflatable decelerator technology as an alternative to or in addition to the aeroshell, where a large structure can remain deflated and stowed away during most of the mission until it is deployed. The toroidal ballute concept, the subject of this investigation, envisions ballutes, which are large enough to allow the spacecraft shock wave to pass through their open center. A spacecraft ballute system is schematically depicted in figure 1. The primary objective here is understanding and insight into the physics, ensuring the functional simplicity of the algorithm and recognizing the essential aspects of the phenomenon significant for wide applications.

Two design reference missions, the Titan Explorer and the Neptune Orbiter are analyzed in the present study. Radiation from a strong shock layer to a blunt body can in general be significant when CN gas products are present in high concentrations. Titan's atmosphere is more than 98 percent Nitrogen, but contains minor amounts of Carbon, while Neptune's atmosphere contains no Nitrogen. In this study, the essentially cylindrical local geometry is open to free gas flow and is not likely to produce significant amounts of CN or shock layer radiation at the stagnation region of the membrane. Calculations associated with gas composition, state and spectral radiation exchange are beyond the scope of the present study. Radiation from the shock layer is, therefore, assumed to be negligible and the secondary shocks effects associated with riser cables are assumed to be insignificant. The critical thermal consideration here is the temperature attained at the stagnation point of the membrane material.

Aerocapture Ballutes

Aerocapture ballutes, a form of Inflatable Aerodynamic Decelerators (IAD), are large area structures and lack the maneuvering capabilities of aeroshells, since they can produce relatively little lift. They are deployed at high altitudes in a planetary body's atmosphere to perform deceleration due to their high drag, and are structurally and thermally less robust than aeroshells. Although they have been investigated since the late nineteen sixties [2-4], they are in the early stages of technology development. One of the challenges is the survival of the lightweight ballute material from a mechanical, as well as, from a thermal point of view. Toroidal ballutes have been proposed, which are tethered to the spacecraft, inflated and later released after sufficient entry velocity has been lost to enable aerocapture. A toroidal system can be designed such that all flow processed by the bow shock of the towing spacecraft, ignoring influence of the tethers, passes through the hole in the toroid. Significant progress has been made in manufacturing of ballute materials, aerothermal analysis, trajectory control, and aeroelastic modeling. Stowing the ballute and its release are doable, but the dynamic stability of the spacecraft-ballute system is a more challenging problem. These topics, however, are outside of the scope of the present research, since gaining insight into the thermal problem is the primary goal here.

Several considerations must be made in choosing the materials for ballute membrane. Clearly the internal pressure for inflating and maintaining a certain degree of structural in-

tegrity is a factor. Ballutes can be inflated in vacuum prior to atmospheric interface. The inflation pressure, depending on the structural design of the ballute, must prevent large geometrical deformations during maximum drag. Critical membrane tensile strength is approached when substantial atmospheric and aerodynamic forces are encountered. The critical membrane tensile strength, however, is a function of temperature. The membrane and internal gas temperatures must, therefore, be taken into account in the deployment sequence.

A number of commercially available materials have been suggested for various preliminary considerations [5-7]. They appear to be generally non-metallic and mostly polymeric in nature, such as Kapton, Polyester and Polyethylene. Some contain multiple components, for example, fabrics for tensile strength and coatings to render them impermeable. A common theme between most of them is that they use a single layer of thin materials referred to as thin films. Some of these materials are capable of maintaining sufficient integrity up to temperatures of several hundreds of degrees Kelvin.

Ballute Thermal Problem

Clearly large ballutes cannot be successfully designed to contain rigid or massive structures. They will be analogous to thin membrane balloons laced with cables and only capable of withstanding moderate accelerations and temperatures. The spacecraft and ballute must develop a significant amount of drag, while minimizing heat flux. Convective aerothermal heating rates are kept to low levels so that heat can be radiated away without ablation at the surface. In general an extensive model of an aerocapture ballute would likely involve non-axisymmetric computation of the external flow field including the spacecraft flow field and possible shock layer radiation. Entry conditions exist where radiative heating may be an important contributor to the total heat load, for example, entry into the earth's atmosphere at Mars return velocities and flight under low-density non-equilibrium conditions during the aerocapture maneuver [8]. Non-equilibrium radiation can be present even when equilibrium radiation is insignificant. Magin, Caillault, Bourdon and Laux [9] have presented radiative heat flux predictions of Huygens probe during entry into Titan's atmosphere based on the solution of the radiative transport equations in thermo-chemical non-equilibrium. The radiative heating during the entry is primarily due to the CN system. Computation of shock layer radiation, however, is rather involved and is outside the scope of the present report. The problem is further complicated by possible coupling of multi dimensional convection heat transfer in the inflation gas due to oscillations in addition to radiation [10-11]. Oscillations and free convection due to temperature gradients in the inflation gas are assumed to not be present or be negligible due to stable fluid stratification.

Free molecular and transitional flow regimes appear to constitute favorable conditions for this concept, depending on the trajectory and attitude stability that the ballute and the spacecraft can tolerate. Continuum flow regime poses more severe demands on the mechanical integrity of the system. Feasibility of the concept under these conditions has not yet been established. The aforementioned conditions are external to the ballute, while ballute surface radiation and the inflating gas heat transfer processes may be considered internal and surface controlled. Analyses of the internal heat transfer problem have not been

reported in the literature, although heat transfer to the inflating gas and radiation from the interior surfaces must be assessed in the advanced stages of the program as part of a high fidelity research and development effort. The stagnation point of a toroidal ballute is subjected to spatially maximum aerodynamic heating and is the most likely region to fail due to over temperature conditions. Since toroidal ballutes are symmetric and typically have large diameters in comparison to the diameter of the circle of revolution, only a cross section of the circle of revolution needs to be considered.

The Computational Fluid Dynamics (CFD) results of Gnoffo [12] for the external flow field and the results of computations of Hall and Le [11] for two reference missions produced the set of mission parameters employed here. They are presented in a later section. The two missions, as mentioned earlier, are the Titan Explorer and the Neptune Orbiter. These mission parameters are used as a basis for the present study. Heat transfer to the membrane at the stagnation point and the internal heat transfer along a local line of symmetry through the circle of revolution are the focus of the present model.

THERMAL MODEL

The present model is an approximation of the transient response at the flow stagnation point, employing a two-dimensional methodology, where conduction resistance in the material and convection in the gas are neglected. The transient nature of this problem stems from two distinct factors. Firstly, the trajectory considerations impose a varying free stream velocity and density and thus varying heat input. Secondly, the finite mass of the inflation gas is heated or cooled throughout the time period.

As shown in figure 1, an area on the stagnation point of the ballute membrane material is considered. This area is extended into a volume element through the inflation gas to the opposite side of the ballute ring, parallel to the free stream flow. The ballute ring has a radius, r and the free stream flow is at a velocity, U_∞ . Since the membrane is very thin and despite its relatively low thermal conductivity and finite heat capacity, we can assume that it responds to the heat input rapidly and radiates on both sides instantaneously at a uniform, but transient temperature, T_w .

Due to the differing response times of the inflation gas and the membrane, one may consider a quasi-steady conduction and radiation heat balance situation. One may choose a small time step, Δt during which the temperature of the inflation gas is almost unchanged. For the initial time step, a balance between radiation and aerothermal convection heat input, q_a can be assumed according to the Stefan-Boltzmann law.

$$(1) \quad q_a = 2 \epsilon \sigma T_w^{**4}$$

For the present model we approximate the gas heating, q_c by considering the gas bulk temperature T_b , increasing according to the conduction of heat to a semi-infinite fluid at rest during the initial time step Δt , as well as, the consequent time steps. We assume that the gas can be treated to be uniformly at the bulk temperature, T_b of the previous time step,

initially for each new time step. The heat input to the gas can be calculated from the heat conduction equation

$$(2) \quad q_c = k(T_w - T_b) / (\pi \alpha \Delta t)^{** 0.5}$$

Here T_w is the equilibrium temperature prevailing in the Ballute material as a result of convective heating, less conduction to the gas, calculated in the prior time step and balanced by the radiative cooling

$$(3) \quad T_w = [(q_a - q_c) / 2 \epsilon \sigma]^{** 0.25}$$

q_a can be calculated from the standard equation for stagnation point convective heating on a blunt body

$$(4) \quad q_a = C (\rho_\infty / r)^{** 0.5} U_\infty^{** 3}$$

The dimensions of C do not correspond to a dimensionless constant, but the dimensions of q_a are as set forth in the nomenclature. Clearly the trajectory imposes a varying free stream velocity and density. For or a given ballute, the heat input is a function of the velocity for the particular altitude and density.

Reference [11] derived the values of constant C from the two dimensional cold wall formulation aerothermal simulations of reference [12-13]. The velocity and density are supplied by the trajectory calculations.

C= 1.92 E - 4 for Titan Explorer

C= 5.80 E - 5 for Neptune Orbiter

The overall heat transfer to the gas can be calculated from numerical integration of the inflation gas conduction heat flux, q_c over the time steps. The properties and the pressure of the inflation gas are currently not specified, however a good candidate may be Helium, due to its high thermal conductivity and low density. Helium is often used by as an attitude control gas and can be stored at very high pressure in vessels. Helium does not participate in the radiative process and the radiation from the far side of the ballute wall is essentially negligible due to the fourth power dependence of surface radiation. A model algorithm is shown below, using the variables listed in the nomenclature, where Δt represents a uniform time step. In a later section verification and testing of the present model will be discussed

$$t = n \Delta t ;$$

For $n = 0$:

$$T_b(0) = T_i$$

$$q_c(0) = 0.0$$

$$q_a(0) = C (\rho_\infty(0) / r)^{** 0.5} U_\infty(0)^{** 3}$$

$$T_w(0) = [q_a(0) / 2 \epsilon \sigma]^{** 0.25} ;$$

Note that T_i may be different than T_∞ and can be much higher if the ballute needs to be warmer than the extremely cold free stream temperature to allow deployment.

For $n > 0$:

$$q_c(n) = k (T_w(n-1) - T_b(n-1)) / (\pi \alpha \Delta t)^{** 0.5}$$

$$q_a(n) = C (\rho_\infty(n) / r)^{** 0.5} U_\infty(n)^{** 3}$$

$$T_w(n) = [(q_a(n) - q_c(n)) / 2 \epsilon \sigma]^{** 0.25}$$

$$T_b(n) = T_b(n-1) + \Delta t q_c(n) / 2 r \rho c_p$$

A number of other effects may come into play when considering the real world manifestation of this concept. The assumption of temperature uniformity in the membrane can be removed by considering the heat conduction and heat capacity of the material. However, removal of this idealization only marginally improves the accuracy of the results, as compared with other factors. The ballute wind ward heating drops off with increasing angle from the stagnation point around the ballute ring, but it has no effect on the results due to symmetry of the problem on the plane of symmetry. That is, derivatives in the lateral direction and therefore lateral conduction vanish as the stagnation point is approached. Alternatively the same is true due to the relative thinness of the membrane compared to its essentially infinite lateral dimensions. Lateral conduction in the inflation gas also does not come into play, when the stagnation point is considered. However, more critical issue may come into play, if significant interactions between shock waves from the tow cables with the boundary layers were present.

As pointed out earlier, in cases where the heat flow to the inflation gas is negligible for all time steps, a model balancing the aerodynamic heating with surface radiation is achieved. The surface temperature can then be simply calculated from the following equation.

$$T_w(n) = [C (\rho_\infty(n) / r)^{** 0.5} U_\infty(n)^{** 3} / 2 \epsilon \sigma]^{** 0.25}$$

TRAJECTORY FOR AEROCAPTURE

The trajectories for aerocapture of the missions for the Titan Explorer and Neptune Orbiter were calculated utilizing the Traj code [15]. Traj is a computer program used for design of TPS for direct atmospheric entry and aerocapture trajectories using a three degrees of freedom trajectory simulation program. Stagnation point heat transfer can also be calculated in Traj, but only for nose bodies with insulated walls, as opposed to the body section with un-insulated walls of the present geometry.

It is necessary to consider actual mission scenarios to identify realistic atmospheric entry conditions. By selecting combinations of departure and entry conditions and estimating the mission total weight requirements, representative or baseline missions, can be considered. As indicated earlier, reference [11] considers several candidate missions and includes a set of mission parameters to Titan and Neptune, the Titan Explorer and the Neptune Orbiter. The values for the vehicle mass, initial velocity, altitude and entry angle, the ballistic coefficient and diameter of the circle of revolution of ballute ring are tabulated below:

	Titan Explorer	Neptune Orbiter
Vehicle mass, kg	393	335
Initial Flight Angle, degrees	-34.3	-10.8
Initial Vehicle speed, km / s	9.6	28.7
Initial Vehicle Altitude, km	1,200	1,200
Ballistic Coefficient, kg / m ²	0.63	0.36
Circle of Revolution Diameter, m	13	25

Achieving aerocapture for the present mission parameters is not a trivial matter, although aerocapture conditions do exist when precise mission parameters are calculated and are truly reached. Trajectory calculations based on these values were carried out using the Traj code [15]. For the Titan Explorer an entry angle of -34.3 degrees and for the Neptune Orbiter an entry angle of -10.8 degrees produced aerocapture. The velocity data as a function of time from the initial conditions are presented in figure 2. The trajectories are sensitive to the values of the entry angle for the initial conditions imposed as noted by reference [11]. Traj exhibited a narrower aerocapture entry corridor than was reported in reference [11]. In both cases, high values for the entry angle produce impact conditions, while low values produce skip off conditions. The sensitivities are of considerable importance to the orbital dynamics problem, which is outside the scope of the present research. They also alter the heat transfer, which make very precise comparisons unwarranted, unless extensive future studies are conducted.

HEAT TRANSFER RESULTS

The free stream velocity, temperature and density as functions of time were extracted at uniform time intervals from the trajectory solutions and were used as input data in the thermal model algorithm described earlier. The initial free stream atmospheric temperatures for the Titan Explorer and the Neptune Orbiter missions were 175 K and 148 K respectively. The values for the emissivity for the membrane were set at 0.9, representative for the material under consideration, while the inflation gas heat capacity, thermal conductivity and thermal diffusivity were $1.4E4$ J/kg-K, 0.2 W/m-K and $1.55E-04$ m²/s respectively. Owing to the relatively large volume of the inflation gas, its pressure and temperature are expected to remain only slightly above atmospheric values.

The model calculated the convective, conductive and radiative heat transfer for the stagnation point and the inflation gas. The convective heat transfer results are presented in figure 3. As showed therein, the maximum convective heating occurs at 180 seconds and at 230 seconds for the Titan Explorer and the Neptune Orbiter missions respectively. The membrane temperature at the stagnation point is presented in figure 4. The maximum membrane temperature occurs at the above times and reaches values of 780 K and 839 K for the Titan Explorer and the Neptune Orbiter missions respectively. The bulk temperature of the inflation gas, as shown in figure 5, increased only of order 20 K for both missions, indicating that the initial gas temperature is more important in determining the final gas temperature than conduction during reentry. As indicated earlier, these temperatures may be too low for proper deployment of stowed ballutes. If higher temperatures are needed, the algorithm allows these values to be set to higher temperatures.

In a simpler model, reference [11] assumed a balance between radiation from one side of the membrane and aerothermal convection according to the Stefan-Boltzmann law. In that study conduction to the inflation gas and radiation from the inner surface of the membrane were ignored. The results presented in reference [11] indicate that the maximum membrane temperature for the Titan Explorer and the Neptune Orbiter missions occur at approximately 170 and 200 seconds and reach mean values of 1052 K and 1327 K respectively. These maximum temperatures are reached approximately 10 and 30 seconds earlier than those predicted in the present study for the Titan Explorer and the Neptune Orbiter missions respectively.

As noted earlier, there are differences between the trajectory sensitivities and therefore the actual trajectories for the present report and those used in reference [11]. Although aerocapture is achieved in both studies for similar initial entry conditions, since the density and velocity conditions encountered have sharp gradients, the aero heating and heat transfer are also sensitive to the exact conditions of the trajectory. The membrane temperatures in both studies are in reasonable agreement, but they cannot be compared precisely unless a more extensive study of the trajectory problem is conducted. The present study, however, was extended by computations with analogous physical modeling to reference [11], i.e. without conduction through the membrane and having radiation only on one side. The wall temperatures achieved, also presented in figure 4, for Titan Explorer and the Neptune Orbiter missions occur again at approximately 180 and 230 seconds and reach mean values of 937 K and 1007 K respectively, showing a favorable trend in approaching the results reference [11].

VERIFICATION

It should be noted that the computational algorithm presented here was tested to verify its validity. Exact or approximate analytical solutions for the problem at hand do not exist, however there are solutions available in the heat transfer literature for some limiting cases, which are both physical and are of interest for application to spacecraft. The first case considered is for insulated wall, i.e. where the conductivity of the inflation gas is negligible or set to zero. This case approximates a non-ablative, but highly insulating thermal protection material used in a reentry environment, where the aerothermal heating is balanced by surface thermal radiation. The surface temperatures obtained from the present algorithm for this case very closely matched the values obtained using the Stefan-Boltzmann law.

The second test case considered is for constant values of the free stream velocity and density, which imposes constant convective heating at the surface. Conduction to the inflation gas takes place, but the heat transfer processes here are controlled by the highly non-linear surface radiation transfer mechanism. In this case, consistent with the missions considered for the present analyses, the conductive portion of the total heat transfer from the surface was only a few percent, the rest being dissipated by radiation. The free stream velocities and densities were set at arbitrary, but physically realistic middle range values for the tests cases. Although heat transfer literature contains a large number of rigorous analytical solutions involving heat conduction in solids, it is devoid of a suitable or similar case for comparison. The very low heat conduction to the inflation gas for the ballute system, however, allows an approximate comparison of wall temperatures for a purely radiative surface to the values obtained from the present algorithm. For this test case, the surface temperatures obtained from the present algorithm were lower than the values obtained using the Stefan-Boltzmann law by less than three percent, a reasonably expected outcome.

CONCLUSIONS

The present model predicts the approximate peak ballute stagnation point temperatures at roughly the same times as predicted in reference [11], but at somewhat lower values. Aerocapture is achieved in both studies for similar initial entry conditions, but since the density and velocity conditions encountered have sharp gradients, the aero heating and heat transfer are also sensitive to the exact conditions of the trajectory. The wall temperatures in both studies are in reasonable agreement, however, a precise comparison cannot be made unless more extensive studies of the trajectory problem is conducted. The lower temperatures may be a result of the differences in the trajectories and the more realistic two sided radiation boundary conditions set forth in the present study. The temperatures obtain are within the tolerable limits for the membrane materials considered. So far as the internal and surface controlled thermal modeling is concerned, the likely oscillatory nature of the dynamical spacecraft-ballute system poses a challenging mechanical design. The heat transfer is primarily controlled by radiation, although forced convective currents within the inflation gas may be generated, possibly lowering the temperature of the heated area.

In an extension to the present model and depending on the nature and magnitude of the flow field outside and inside the ballute, a quasi-steady aerothermal convective and radiative problem may be constructed, for example for analyses of the Hypersonic or Supersonic Inflatable Decelerators HIAD and SIAD, respectively. In such a model the heat conduction

resistance in the membrane and heat capacity of the membrane material, although of secondary importance, may also be taken into account. These extensions, however, would render the present method more complex, requiring further development.

BIBLIOGRAPHY

1 – J. Masciarelli and R. Rohrschneider, "Summary of Ultralightweight Ballutes Technology Advances", 6th International Planetary Probe Workshop, Atlanta, Georgia, 2008.

2 - I. M. Jahemenko, "Ballute Characteristics in the 0.1 to 10 Mack Number Speed Range", J. Spacecraft. Vol. 4, No. 8, 1058-63, 1967.

3 - L. D. Guy, "Structure and decelerator Design Options for Mars Entry, J. Spacecraft", Vol. 8, No.1, 44-49, 1969.

4 - H. L., Bohon, Sawyer, J. W. and Miserentino, R., "Deployment and Characteristics of 1.5-Meter Supersonic Attached Inflatable Decelerators", NASA-TN-D-7550, 1974.

5 - A. D. McDonald, "A light Weight Inflatable Hypersonic Drag Device for Venus Entry, AAS/AIAA Astrodynamics Specialist Conference", Girdwood, AK, 1999.

6 - A. D. McDonald, "A light Weight Hypersonic Inflatable Drag Device for a Neptune Orbiter", AAS 00-170, AAS/AIAA Space Flight Mechanics Meeting, Clearwater, FL, 2000.

7 - A. Yavrouian, S.P.S. Yen, G. Plet, and N. Weissman, "High temperature Materials for Venus Balloon Envelops", Jet Propulsion Internal Report, 1995

8 - W. C. Davy, C. Park, and J. O. Arnold, "Radiometer Experiment for the Aeroassist Flight Experiment," AIAA Paper 85-0967 (1985).

9 - Magin, T., Caillault, L., Bourdon, A., and Laux, C., "Nonequilibrium radiative heat flux modeling for the Huygens entry probe," Journal of Geophysical Research-Planets, Vol. 111, No. E7, 2006, pp. E07S12.

10 - J. L. Hall, "A Review of Ballute Technology for Planetary Applications, 4th IAA Conference on Low Cost Planetary Missions", Laurel, MD, 2000.

11 - J. L. Hall and A. K. Le, "Aerocapture Trajectories for Spacecraft with Large, Towed Ballutes", AAS/AIAA Space Flight Mechanics Meeting, Santa Barbara, CA, 2001.

12 - P. A. Gnoffo, "Computational Aerothermodynamics in Aeroassist Applications", AIAA paper 2001-2632, 2001.

13 - P. A. Gnoffo, Brian P. Anderson, "Computational Analysis of Towed Ballute Interactions" AIAA Paper 2002-2997, 8th AIAA/ASME Joint Thermophysics and Heat Transfer Conference, Saint Louis, MO, 2002.

14- D. Way, R. Powell, K. Edquist, J. Masciarelli, B. Starr, "Aerocapture Simulation and Performance for the Titan Explorer Mission," AIAA-2003-4951, AIAA/ASME/SAE/ASEE Joint Propulsion Conference, Huntsville, AL, July 2003.

15 - Gary A. Allen, Jr., Michael J. Wright and Peter Gage, "The Trajectory Program (TRAJ): Reference Manual and User's Guide", NASA/TM-2005-212847, March 2005.

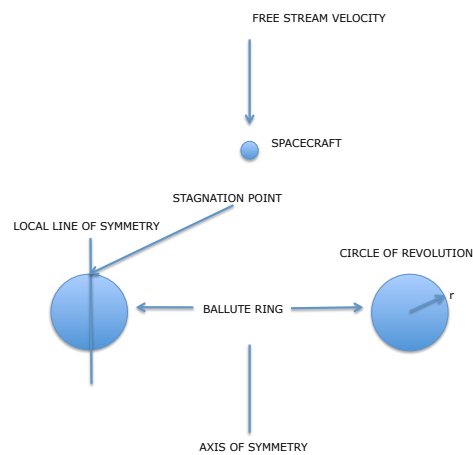


FIGURE 1

Figure 1. Schematic representation of the spacecraft-ballute system

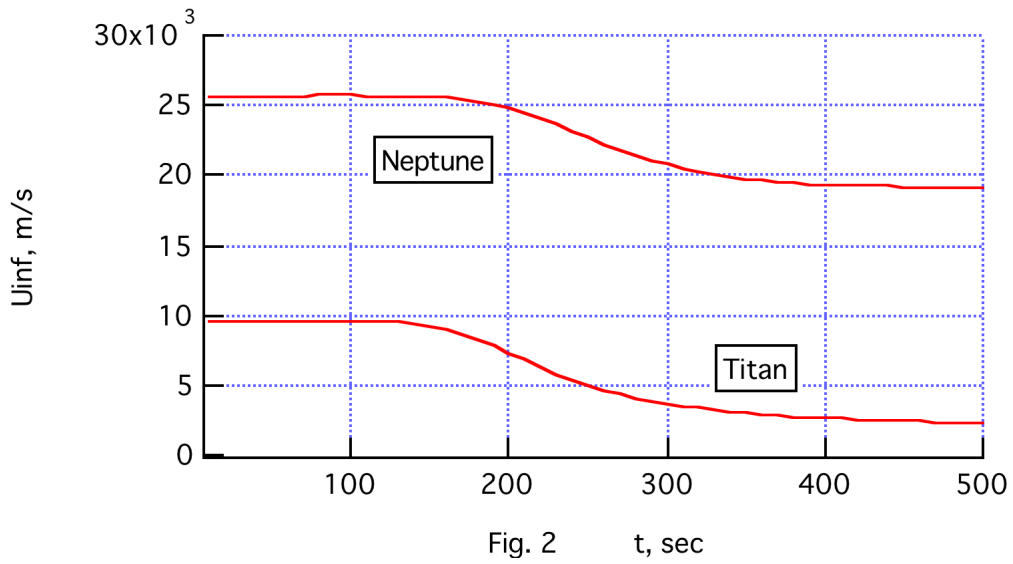


Figure 2. Free-stream velocity as a function of time from the initial conditions

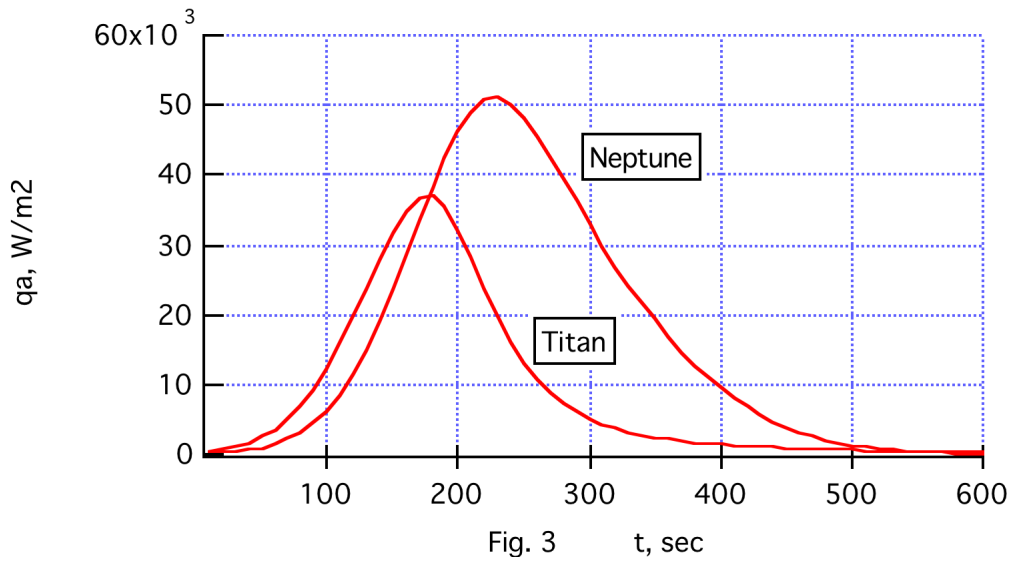


Figure 3. Convective heat transfer as a function of time

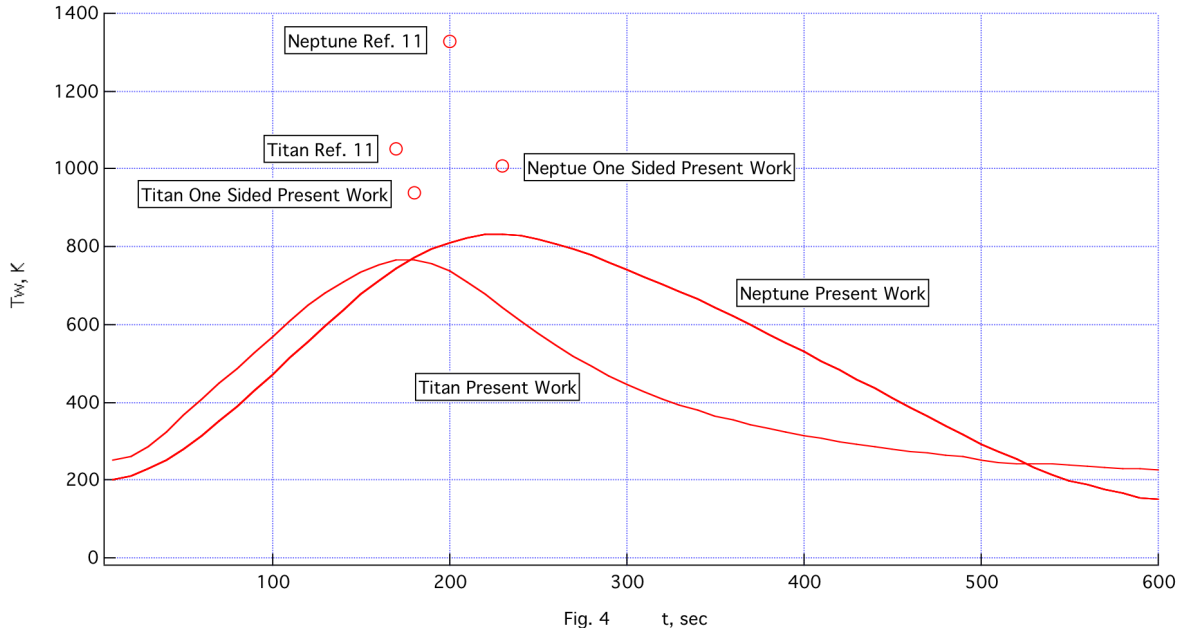


Fig. 4 t, sec

Figure 4. Membrane temperature at the stagnation point

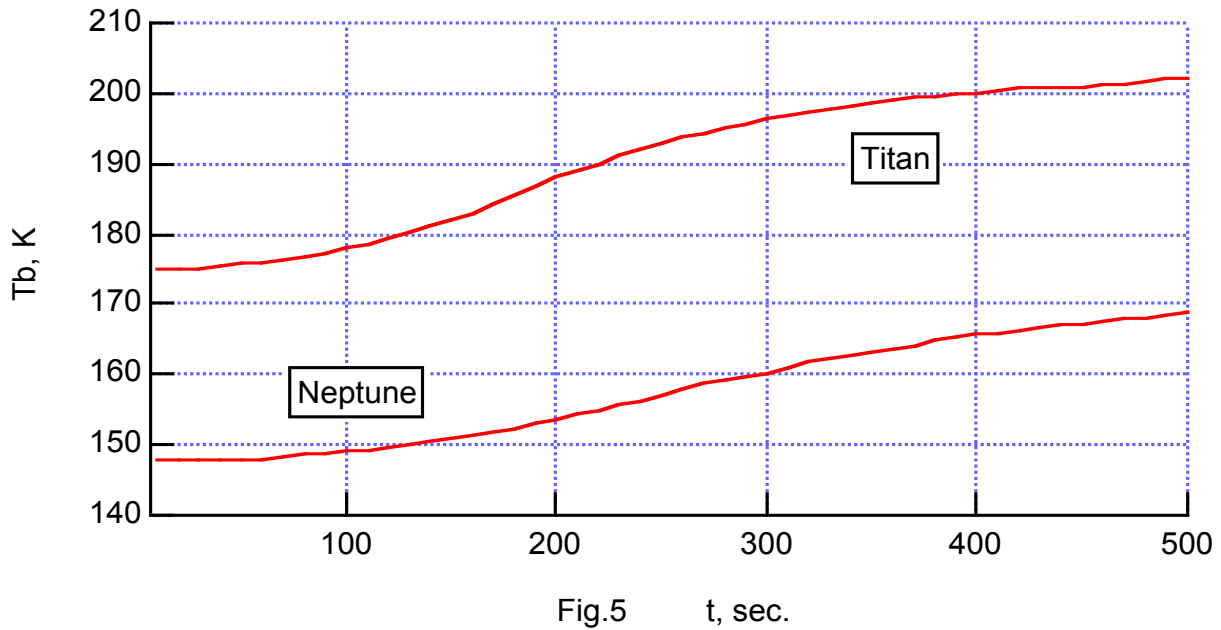


Fig.5 t, sec.

Figure 5. Bulk temperature of the inflation gas